

CORDIERITE-PRODUCING REACTIONS IN THE PEÑA NEGRA COMPLEX, AVILA BATHOLITH, CENTRAL SPAIN: THE KEY ROLE OF CORDIERITE IN LOW-PRESSURE ANATEXIS

MARÍA DOLORES PEREIRA*

*Departamento de Geología, Area Petrología y Geoquímica, Universidad de Salamanca,
Plaza de la Merced s/n, 37008 Salamanca, Spain*

FERNANDO BEA

*Departamento de Mineralogía y Petrología, Facultad de Ciencias, Universidad de Granada,
Fuentenueva s/n, 18002 Granada, Spain*

ABSTRACT

By studying the low-pressure Peña Negra migmatites, associated with the Avila batholith, in central Spain, we were able to identify what mineral reactions produced the different textural varieties of cordierite (metamorphic-, magmatic- and retro-metamorphic-looking) commonly occurring in these rocks, and what role cordierite played in the low-pressure anatexis. Cordierite was not produced by the incongruent melting of biotite, but at subsolidus conditions by the continuous reaction: 0.96 biotite + 0.40 sillimanite + 0.33 quartz = 1.00 cordierite + 0.30 [higher-Ti and higher-Fe/(Fe+Mg)] biotite + 0.36 K-feldspar + 0.01 ilmenite + 0.03 water. When this reaction occurred in the presence of melt, normally zoned, magmatic-looking subidiomorphic crystals were formed. Large, inversely zoned, more magnesian crystals grew from the melt either on inherited crystals or from new nuclei. These processes happened sequentially as a result of advancing anatexis. Retrogression of garnet produced cordierite through the continuous reaction: 2.13 biotite + 1.38 garnet + 0.35 sillimanite + 0.09 quartz + 0.09 albite (from plagioclase) = 1.00 cordierite + 2.25 [lower-Ti and higher-Fe/(Fe+Mg)] biotite + 0.72 (higher-Mn and lower-Mg) garnet + 0.05 ilmenite + 0.001 anorthite (to plagioclase). At low pressures, the P-T path has a great influence on melt productivity. Within the temperature range of 660–750°C, rocks that evolve along a pressure path low enough to intercept the invariant biotite + sillimanite + quartz = cordierite + K-feldspar + water at subsolidus conditions are more fertile than those evolving at higher pressure, although the chemical composition is the same. The presence of cordierite in source rocks increases their fertility in two ways: (1) directly, due to congruent melting at low temperature in the presence of quartz and K-feldspar, and (2) indirectly, because cordierite-producing reactions release water and increase the percentage of the haplogranitic component in the anatectic system through the release of K-feldspar.

Keywords: Peña Negra anatectic complex, migmatite, anatexis, cordierite-producing reactions, garnet breakdown, Spain.

SOMMAIRE

Suite à notre étude du complexe migmatitique de Peña Negra, associé au batholite d'Avila, en Espagne centrale, nous avons réussi à identifier les réactions impliquant les diverses variétés texturales de cordiérite (métamorphique, magmatique, et d'apparence rétrograde) dans ces roches, et à déterminer le rôle qu'a joué la cordiérite dans les réactions anatectiques à faible pression. Nous pouvons éliminer un modèle pour sa formation par la fusion incongruente de biotite; par contre, elle semble causée par une réaction continue à conditions subsolidus: 0.96 biotite + 0.40 sillimanite + 0.33 quartz = 1.00 cordiérite + 0.30 biotite [à teneur en Ti et à rapport Fe/(Fe+Mg) plus élevées] + 0.36 feldspath potassique + 0.01 ilménite + 0.03 H₂O. Là où cette réaction a procédé en présence d'un liquide silicaté, des cristaux sub-idiomorphes normalement zonés, à apparence magmatique, en ont résulté. Des cristaux plus grossiers, inversement zonés et plus fortement magnésiens, ont cru à partir du magma, soit par la croissance continue de cristaux hérités ou par la nucléation de nouveaux cristaux. Ces processus de formation sont apparus en séquence, à mesure que progressait l'anatexie. La déstabilisation du grenat a produit la cordiérite selon la réaction continue: 2.13 biotite + 1.38 grenat + 0.35 sillimanite + 0.09 quartz + 0.09 albite (provenant du plagioclase) = 1.00 cordiérite + 2.25 biotite [à teneur en Ti plus faible et à rapport Fe/(Fe+Mg) plus élevé] + 0.72 grenat (à teneurs plus élevée en Mn et plus faible en Mg) + 0.05 ilménite + 0.001 anorthite (contribution au plagioclase). A faibles pressions, le tracé en termes de P-T exerce une grande influence sur le taux de production de liquide. Dans un intervalle de température compris entre 660 et 750°C, les roches ayant évolué le long d'un tracé à pression suffisamment faible pour favoriser une intersection de la réaction invariante biotite + sillimanite + quartz = cordiérite + feldspath potassique + H₂O sous le solidus seront plus fertiles que celles qui auront évolué à pression plus élevée, malgré leur composition identique. La présence de cordiérite dans les roches sujettes à une réaction anatectique augmente leur fertilité de deux façons, une directe, par sa fusion congruente à température relativement faible en présence de quartz et de feldspath potassique, et l'autre indirecte, résultat du fait que les réactions qui produisent la cordiérite dégagent de l'eau et augmentent la proportion de la fraction haplogranitique dans le système anatectique par la déstabilisation du feldspath potassique.

(Traduit par la Rédaction)

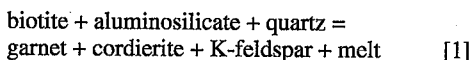
Mots-clés: complexe anatectique de Peña Negra, migmatite, anatexie, formation de la cordiérite, déstabilisation du grenat, Espagne.

* Present address: Department of Geology, McMaster University, Hamilton, Ontario L8S 4M1.

INTRODUCTION

Cordierite is a widespread mineral in anatectic migmatites, where it may appear within the mesosome, the melanosome, or the leucosome. Depending on the pressure that prevailed during partial melting, migmatites may show systematic differences both in the frequency distribution of cordierite among their components, and in the nature and behavior of the associated ferromagnesian silicates.

In cordierite-bearing migmatites formed at pressures greater than 4–4.5 kbar, cordierite is usually restricted to leucosomes, where it always appears associated with garnet (*e.g.*, Ashworth & Chinner 1978, Brown 1983, Tracy & Robinson 1983, Fitzsimons & Harley 1991). In this case, cordierite is generally believed to be generated by the incongruent melting of biotite through a reaction such as:



(*e.g.*, Holdaway & Lee 1977, Thompson 1982, Grant 1985a). Additional support for this idea is provided by the fact that the modal abundance of biotite in the matrix of the mesosome commonly decreases toward the leucosome veins.

On the other hand, migmatites that originated at pressures less than 4–4.5 kbar commonly have cordierite in both the mesosome and the neosome, although of different textural varieties (*e.g.*, Jamieson 1984, Perreault & Martignole 1988, Vernon *et al.* 1990, Pereira 1992). In mesosomes and melanosomes, cordierite appears in granoblastic aggregates, and its modal abundance decreases near the zones of segregation of anatectic melt (Pereira 1992). Leucosomes in such rocks, as well as low-melt-fraction (in terms of Wickham 1987) anatectic granitic rocks, usually contain large, euhedral crystals of cordierite as the dominant femic mineral, with subordinate biotite and no garnet. Restites, however, are rich in biotite or sillimanite (or both), but devoid of cordierite (*e.g.*, Bea 1991). This situation contrasts with what happens at higher pressures, and precludes an origin for cordierite through the incongruent melting of biotite, at least by the mechanism conveyed by equation [1]. The availability of cordierite at the beginning of anatexis, together with the possible effect of cordierite in lowering the solidus temperature in haplogranitic systems at low pressure (Grant 1985a, b), led us to suspect that given the appropriate conditions, cordierite could play a more active role during low-pressure anatexis than previously suspected.

Here we present the results of an extensive electron-microprobe survey of cordierite and associated minerals from a typical example of low-pressure anatexis, the Peña Negra Complex in Spain, where cordierite is ubiquitous in both migmatites and anatectic

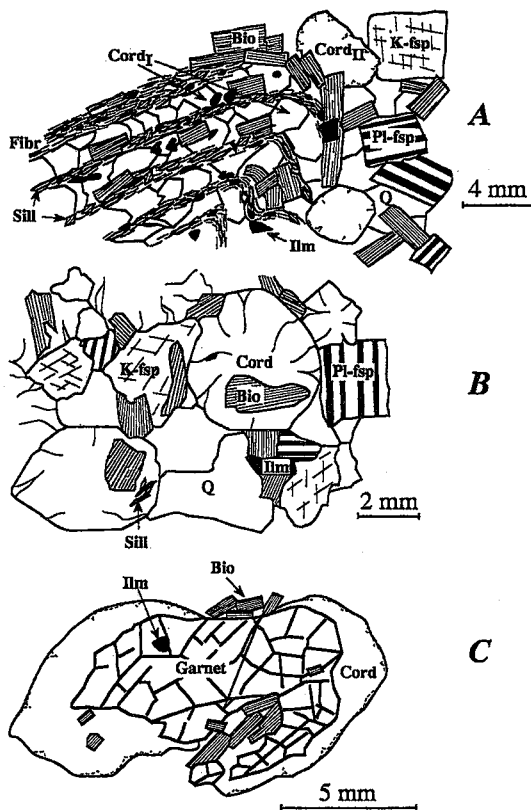


FIG. 1. Textural varieties of cordierite in Peña Negra anatectites. A. Melanosome with metamorphic cordierite (Cord_I) cut by leucosome with type-II magmatic cordierite. B. Magmatic, type-III cordierite crystals in a subautochthonous granodiorite. C. retrograde cordierite surrounding a large crystal of garnet.

granitic rocks, appearing as three distinct textural varieties (Fig. 1) that were probably generated by different reactions: 1) small granoblastic, anhedral crystals with a "metamorphic" appearance, which are specific to restites and migmatite melanosomes, 2) large euhedral or subhedral, locally poikilitic crystals with a "magmatic" appearance; this variety is, by far, the most abundant, and characteristically occurs within migmatite leucosomes and granitic rocks of anatectic origin; 3) anhedral crystals of apparent retrograde origin, that form a rim around the rare crystals of garnet.

This study had a dual purpose: firstly, to identify through mass-balance calculations the nature, modal proportions, and compositional variations of minerals involved in the reactions that produced each textural variety of cordierite, and secondly, to assess the role of cordierite in low-pressure anatexis in peraluminous systems.

ANALYTICAL METHODS

The chemical composition of minerals was obtained by wavelength-dispersion analysis with CAMECA electron microprobes at the Universities of Oviedo (Spain) and Padova (Italy) using synthetic standards. In both cases, the accelerating voltage was 15 kV, and the sample current, 10 nA. Precision is within $\pm 2\%$ for major and $\pm 5\%$ for minor elements, respectively. Whole-rock major-element determinations were done by Inductively Coupled Plasma – Optical Emission Spectrometry (ICP–OES) after digesting 0.2 g of sample powder with $\text{HNO}_3 + \text{HF}$ under pressure in a Teflon-lined vessel at controlled temperature. Instrumental measurements were carried out in triplicate with a Perkin–Elmer Plasma II spectrometer using the Myers–Tracy signal-compensation system. Typical precision was about $\pm 0.25\%$ rel., $\pm 0.75\%$ rel. and $\pm 2.5\%$ rel. for analyte concentrations of 10, 1, and 0.1 wt%, respectively.

GEOLOGICAL BACKGROUND

The Peña Negra Anatectic Complex (Bea & Pereira 1990, Pereira 1993) crops out over 350 km² in the central part of the Gredos sector of the Hercynian Avila Batholith, central Iberian Variscan Belt. It is composed of low-pressure migmatites and related anatectic granitoid rocks, which have cordierite + biotite as the prevalent ferromagnesian mineral assemblage (Bea 1982).

The regional rocks at Peña Negra are diatexitic migmatites, customarily called “mesocratic mig-

matites”, with a granodioritic composition and no recognizable mesosome. They form a thick series of more than 1000 m of vertical exposure. Intimately associated with the mesocratic migmatites are several types of anatectic granitoid rocks, classifiable in two groups: subautochthonous granodiorite and cordierite-bearing leucogranite (Fig. 2). The subautochthonous granodiorite grouping (Rb/Sr age $\approx 310 \pm 6$ Ma, initial $^{87}\text{Sr}/^{86}\text{Sr} \approx 0.7096$; Pereira *et al.* 1992) occurs as large, subhorizontal, concordant sheets and includes porphyritic, cordierite-bearing granodiorite and monzogranite that grades transitionally into mesocratic migmatites, having almost the same chemical and isotopic composition as these. Cordierite-bearing leucogranite (Rb/Sr age in the range 305–295 Ma, initial $^{87}\text{Sr}/^{86}\text{Sr} \approx 0.7111$, unpublished data of authors) occurs as small bodies whose geometry ranges from narrow veins of leucosome to lens-shaped dikes and irregular autochthonous plutons (maximum diameter 40 m) with transitional contacts to the mesocratic migmatites. Both kinds of granitic rocks were generated from the same source, the mesocratic migmatites, but at different degrees of partial melting. The subautochthonous granodiorites are high-melt-fraction granitic rocks with little or no separation of restite, whereas the cordierite-bearing leucogranites represent a low-melt-fraction granite with a limited restitic component (Bea 1991, Pereira 1989, 1992).

PETROGRAPHY

Pereira (1989) classified the mesocratic migmatites into three types according to their mesoscopic struc-

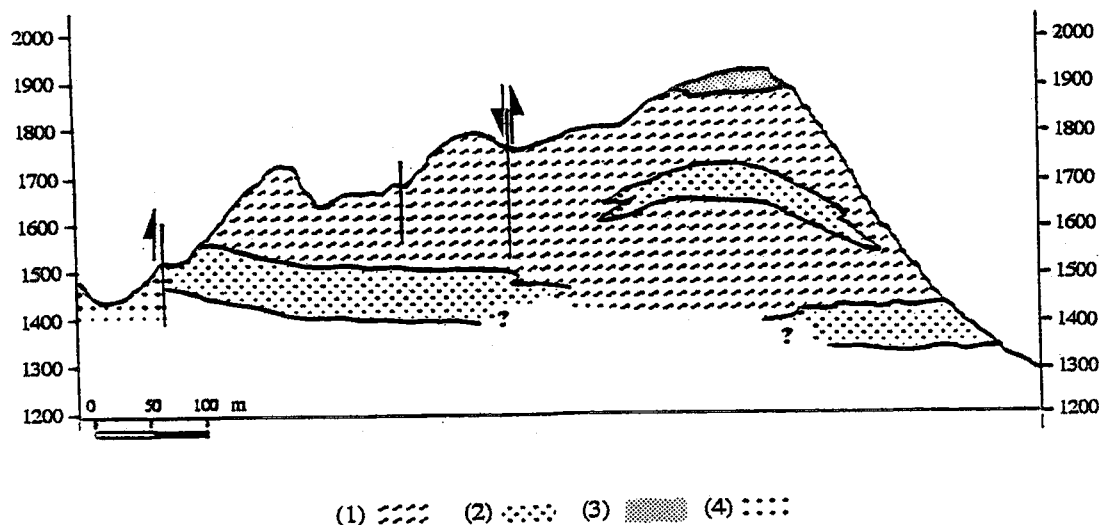


FIG. 2. Schematic section of Peña Negra Anatectic Complex, showing the main rock-types: 1 migmatite, 2 granodiorite, 3 leucogranite, and 4 Hercynian granites surrounding the Complex.

tures: (1) schlieren, (2) nebulitic, and (3) transitional (to the subautochthonous granodiorites). The three types have almost the same bulk mineralogical and chemical composition. The schlieren and nebulitic variants differ only in the geometrical relationships between leucosome and melanosome. The transitional rocks are invariably located between the subautochthonous granodiorite and the nebulitic suite, and are characterized by the development of large megacrysts of K-feldspar. The leucosome of the mesocratic migmatites has a hypidiomorphic texture and is composed of quartz + plagioclase (core An_{33-18} , outer rim An_{18-12}) + cordierite + biotite + K-feldspar, with accessory sillimanite, apatite, ilmenite, zircon, pyrite, graphite, monazite, xenotime and, occasionally, tourmaline. Cordierite invariably seems primary; the subhedral untwinned crystals range from 2 to 15 mm across. They usually contain inclusions of drop-like quartz, ilmenite, pyrite, zircon and, less commonly, biotite and sillimanite. The melanosome is composed of layers alternately granoblastic (metamorphic-looking cordierite \pm quartz \pm plagioclase \pm K-feldspar) and schistose (sillimanite + biotite + ilmenite \pm cordierite). In some areas, the mesocratic migmatites, mainly of schlieren type, feature large (maximum diameter in the range 5–40 mm) euhedral or subhedral crystals of almandine-rich garnet, which are invariably surrounded by a rim of low-Mg, retrograde cordierite and biotite crystals (Pereira 1992). The modal compo-

TABLE 1. MODAL COMPOSITION OF MAIN PEÑA NEGRA LITHOTYPES

	Migmatites				Anatectic Granitoids			
	leucosome (11)		melanosome (5)		granodiorites (14)		leucogranites (7)	
	mean	range	mean	range	mean	range	mean	range
Qtz	29.2	24.3-31.0	3.5	1.2-10.3	29.1	27.6-30.2	31.7	30.8-32.8
Kfs:	12.0	7.0-15.2	traces		10.7	9.1-15.0	31.96	26.4-35.1
Plg:	29.3	28.3-30.2	5.7	3.2-9.2	35.2	28.4-37.5	27.6	24.3-30.0
Bt:	13.9	11.7-20.1	45.2	37.7-62.8	17.7	10.2-18.9	1.7	0.7-5.2
Crd:	14.5	9.4-19.6	19.7	11.5-25.5	6.9	2.3-9.8	6.8	4.6-8.2
Sil:	0.3	0-0.8	22.8	19.3-30.0	traces		traces	
Ilm:	0.4	0.3-0.6	1.9	0.9-3.5	0.4	0.3-0.6	0.2	0.2-0.3
Ap:	0.3	0.2-0.4	0.2	0.1-0.3	0.6	0.4-0.8	0.2	0.1-0.3
Other*:	0.2	0.1-0.5	1.0	0.3-3.1	0.2	0.1-0.4	0.2	0.1-0.3

Between brackets is the number of counted thin sections.

* Other minerals are sulfides, garnet, zircon, monazite, xenotime, and graphite.

sition of leucosome and melanosome of mesocratic migmatites is shown in Table 1.

The samples of subautochthonous granodiorite have a hypidiomorphic granular texture, with prominent K-feldspar megacrysts (maximum diameter in the range 10–15 mm) and large (maximum diameter in the range 5–25 mm) euhedral crystals of cordierite, variably pinnitized. They are composed (Table 1) of anhedral crystals of quartz, subhedral crystals of zoned plagioclase (core An_{33-29} , outer rim An_{18-12}), crystals of aluminous biotite defining a microsclieren texture, K-feldspar (mostly orthoclase megacrysts), and euhedral or subhedral crystals of cordierite, which are texturally identical to the largest primary crystals from

TABLE 2. MAJOR ELEMENT COMPOSITION, CIPW NORM AND PARAMETERS OF SELECTED SAMPLES FROM PEÑA NEGRA LITHOTYPES

	Migmatites				Granodiorites				Leucogranites			
	1	2	3	4	5	6	7	8	9	10	11	12
Major element composition (wt. %)												
SiO ₂	66.65	62.98	65.22	64.32	68.01	65.45	65.48	64.63	72.14	71.77	71.45	76.34
TiO ₂	0.86	0.75	0.79	0.85	0.62	0.95	0.98	0.59	0.39	0.37	0.23	0.19
Al ₂ O ₃	15.60	17.30	17.22	16.31	15.02	15.69	16.15	17.75	13.97	14.67	14.83	13.11
Fe ₂ O ₃	1.26	n.d.	0.30	n.d.	n.d.	n.d.	0.90	n.d.	0.39	0.28	n.d.	n.d.
FeO	4.39	4.84	4.52	4.94	2.98	4.72	4.68	4.14	1.32	1.63	1.80	1.23
MgO	1.97	2.09	1.95	2.06	0.80	1.72	2.18	1.47	0.74	0.66	0.74	0.53
MnO	0.06	0.08	0.11	0.06	0.03	0.06	0.06	0.06	0.07	0.04	0.04	0.03
CaO	1.35	2.25	1.32	2.34	2.02	2.83	1.76	0.53	1.08	0.82	1.48	0.55
Na ₂ O	2.62	2.71	2.82	3.07	3.02	2.98	2.68	1.65	2.58	2.30	2.77	2.73
K ₂ O	3.59	4.30	4.02	3.19	4.53	3.32	3.60	4.86	5.47	5.40	4.74	3.48
P ₂ O ₅	0.22	0.23	0.11	0.28	0.34	0.35	0.25	0.21	0.25	0.23	0.12	0.20
H ₂ O	1.64	1.89	1.45	2.12	1.63	1.17	1.06	3.56	1.35	1.39	1.37	1.23
Sum	100.21	99.42	99.83	99.54	99.00	99.24	99.78	99.45	99.75	99.56	99.57	99.61
CIPW norm and parameters												
Qtz	30.3	20.4	25.2	24.0	27.2	25.0	27.3	31.9	33.3	35.26	32.5	45.6
Crd	5.5	4.8	6.2	4.3	2.3	2.9	5.3	9.7	2.5	4.18	2.8	4.4
Or	21.5	26.0	24.1	19.4	27.5	20.0	21.5	29.9	32.8	32.50	28.5	20.9
Ab	22.5	23.5	24.2	26.7	26.2	25.7	23.0	14.6	22.2	19.82	23.9	23.4
An	5.3	9.9	5.9	10.1	8.0	12.0	7.2	1.3	3.8	2.61	6.7	1.4
Hy	10.8	13.3	12.0	13.2	6.7	11.7	11.9	10.8	3.5	3.94	4.9	3.4
Ilm	1.7	1.5	1.5	1.7	1.2	1.8	1.9	1.2	0.7	0.72	0.4	0.4
Mag	1.8	—	0.4	—	—	—	1.3	—	0.6	0.41	—	—
Ap	0.5	0.6	0.3	0.7	0.8	0.8	0.6	0.5	0.6	0.56	0.3	0.5
ITT	74.3	70.0	73.6	70.0	80.9	70.7	71.8	76.4	88.3	87.58	84.9	89.9
%An	19.2	29.6	19.6	27.4	23.4	31.9	23.8	8.4	14.6	11.65	21.8	5.6
Fe/(Fe+Mg)	0.61	0.57	0.58	0.58	0.68	0.61	0.59	0.62	0.57	0.62	0.58	0.57

The Fe³⁺/Fe²⁺ ratio was determined by wet chemistry and then applied to the total iron determined by ICP-OES. When the Fe₂O₃ is shown as not determined (n.d.), total iron is expressed as FeO.

the leucosome of mesocratic migmatites. They contain abundant apatite, some sillimanite and zircon, and scarce monazite and xenotime, usually included in biotite.

The samples of cordierite-bearing leucogranite have a medium-grained equigranular hypidiomorphic texture in which euhedral, locally poikilitic crystals of magmatic cordierite (diameter in the range 7–25 mm) are prominent. The essential minerals are quartz, K-feldspar, plagioclase (core An_{25-13} , outer rim An_{12-5}), cordierite and, less abundantly, biotite, which always appears associated with sillimanite in streaks or microsclereren, considered of restitic origin. Apatite, zircon, monazite, and tourmaline appear as accessory minerals. The modal composition is provided in Table 1.

Within anatectic granitic rocks, there are clots or nodules (diameter in the range 3–40 cm), and even metric bodies of restitic material containing biotite, sillimanite, and ilmenite as essential minerals, with accidental quartz and cordierite, invariably defining a metamorphic texture. Many of these bodies have the same textures and mineralogical composition as the melanosome of migmatites, but others are almost monomineralic, composed either of sillimanite or, less commonly, of biotite.

Table 2 shows a selection of chemical compositions of representative rocks from each lithotype.

THE COMPOSITION OF THE ROCK-FORMING MINERALS

Cordierite

Early (pre-microprobe) compilations of compositional data on natural cordierite (Leake 1960, Schreyer 1965) did not lead to meaningful correlations between cordierite chemistry and paragenesis. From more recent compilations of electron-microprobe data, however, it seems that the nature and abundance of channel cations (ChC), Na + K, can be related to paragenesis. Speer (1981), for example, pointed out that magmatic cordierite normally has high Na contents, and Schreyer *et al.* (1990) have proved that high-K cordierite is characteristic of partially molten rocks at very low pressures. Using this approach, we have determined the usefulness of the ΣChC versus $Mg/(Mg+Fe+Mn)$ diagram as a discriminant in a classification scheme by plotting a large dataset of microprobe data of cordierite from very different parageneses and checking whether each paragenetic group defines a different field in the diagram. Figure 3 illustrates how it is possible to discriminate among metamorphic, anatectic, and magmatic cordierite crystals, the value of ΣChC being the most sensitive parameter.

The cordierite from Peña Negra has a moderate $Mg/(Mg+Fe+Mn)$ (in the range 0.40–0.60) and ΣChC (in the range 0.01–0.15 atoms per formula unit, apfu)

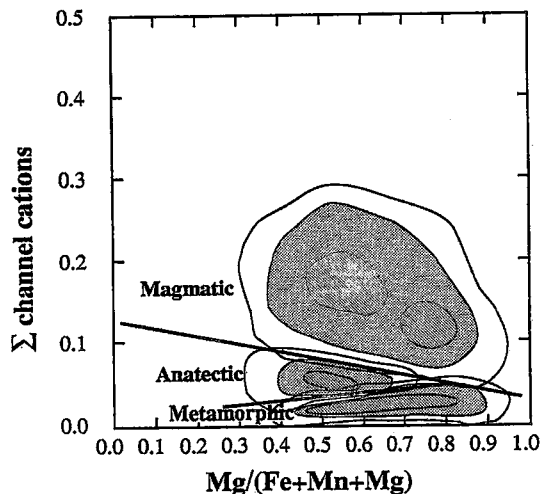


Fig. 3. Classification diagram for cordierite, from data by Lepezin *et al.* (1976), Goldman *et al.* (1977), Speer (1981), Ibaruchi & Martínez (1982), Gervilla (1990), Holtz (1989), Rottura *et al.* (1989), Schreyer *et al.* (1990), Vry *et al.* (1990), Secchi *et al.* (1991), Bea & Pereira (this work and unpublished data). The high- $Mg/(Mg+Fe+Mn)$ maximum is due to cordierite from the Ronda ultramafic complex (Gervilla 1990). Contours show areas where the data are most concentrated in the sample, estimated with the Epanechnikov kernel (Systat 1992).

(Table 3). The projection in the ΣChC versus $Mg/(Mg+Fe+Mn)$ diagram reveals that each textural group has its own compositional identity (Fig. 3). Both metamorphic and retrograde cordierites plot either within anatectic or metamorphic fields, although they differ sharply in $Mg/(Mg+Fe+Mn)$ values (0.44–0.50 versus 0.41–0.44, respectively). On the other hand, data points for magmatic cordierite define the widest range of $Mg/(Mg+Fe+Mn)$ values (0.44–0.58) and plot within anatectic and magmatic fields (Fig. 4).

If the composition of cordierite crystals (except the very rare, garnet-associated variety) from each lithotype is plotted separately in the ΣChC versus $Mg/(Mg+Fe+Mn)$ diagram, the density of data points reveals the existence of four modes or compositional types: Ia, Ib, II, and III (Fig. 5): Cordierite of types Ia and Ib has the same low $Mg/(Mg+Fe+Mn)$ values (<0.49), but different ΣChC (≈ 0.035 and ≈ 0.060 apfu, respectively); cordierite of type II has a $Mg/(Mg+Fe+Mn)$ in the range 0.51–0.53, and cordierite of type III is the most magnesian, with $Mg/(Mg+Fe+Mn)$ greater than 0.54. Most, but not all, crystals belonging to types Ia and Ib have a habit suggestive of a metamorphic origin, whereas practically

TABLE 3. RESULTS OF ELECTRON-MICROPROBE ANALYSIS AND STRUCTURAL FORMULA OF SELECTED CRYSTALS OF CORDIERITE FROM PEÑA NEGRA LITHOTYPES

	Retrograde crystals				Metamorphic crystals								Magmatic crystals							
	1	2	3	4	type Ia				type Ib				type II			type III				
	1	2	3	4	5	6	7	8	9	10	11	12	13	14	15	16	17	18	19	20
Major element composition (wt. %)																				
SiO ₂	47.14	46.78	47.63	47.68	47.83	47.68	47.64	48.48	47.72	47.76	47.96	48.17	46.28	48.11	47.53	47.51	47.87	47.78	48.42	46.36
TiO ₂	0.00	0.03	0.01	0.00	0.01	0.03	0.00	0.00	0.04	0.04	0.02	0.00	0.00	0.05	0.00	0.01	0.00	0.04	0.00	0.04
Al ₂ O ₃	32.42	32.17	31.81	31.83	32.27	32.08	32.05	32.15	32.02	31.97	32.18	31.59	31.94	32.95	31.99	32.50	32.79	32.57	32.79	31.74
FeO	13.76	12.63	12.18	12.63	12.07	11.53	11.96	11.63	11.86	12.05	10.50	11.49	10.09	10.29	9.96	9.92	9.31	8.65	9.83	9.38
MgO	4.32	4.70	4.92	5.30	6.12	5.92	6.10	5.96	5.66	5.99	5.57	6.12	6.19	6.52	6.30	6.43	6.66	6.25	6.93	6.59
MnO	0.10	0.18	0.34	0.41	0.59	0.43	0.23	0.22	0.28	0.29	0.28	0.23	0.28	0.34	0.31	0.24	0.33	0.32	0.26	0.31
CaO	0.05	0.00	0.03	0.03	0.01	0.00	0.00	0.02	0.02	0.06	0.04	0.00	0.02	0.03	0.04	0.05	0.02	0.02	0.00	0.02
Na ₂ O	0.48	0.36	0.41	0.13	0.12	0.17	0.18	0.22	0.27	0.19	0.28	0.25	0.26	0.36	0.30	0.23	0.34	1.18	0.28	0.37
K ₂ O	0.02	0.04	0.04	0.01	0.00	0.00	0.00	0.02	0.00	0.06	0.00	0.00	0.00	0.03	0.03	0.00	0.00	0.03	0.02	0.02
Structural formula based on 18 oxygens																				
Si	4.99	5.00	5.05	5.03	4.99	5.02	5.00	5.05	5.02	5.01	5.06	5.06	4.98	4.99	5.03	5.01	5.01	5.02	5.01	4.99
Al	4.04	4.05	3.97	3.96	3.97	3.98	3.97	3.95	3.97	3.95	4.00	3.91	4.05	4.03	3.99	4.04	4.04	4.04	4.01	4.03
Ti	0.00	0.00	0.00	0.00	0.00	0.00	0.00	0.00	0.00	0.00	0.00	0.00	0.00	0.00	0.00	0.00	0.00	0.00	0.00	0.00
Fe	1.22	1.13	1.08	1.11	1.05	1.01	1.05	1.01	1.04	1.06	0.93	1.01	0.91	0.89	0.88	0.87	0.81	0.76	0.85	0.84
Mg	0.68	0.75	0.78	0.83	0.95	0.93	0.95	0.92	0.89	0.94	0.88	0.96	0.99	1.01	0.99	1.01	1.04	0.98	1.08	1.06
Mn	0.01	0.02	0.03	0.04	0.05	0.04	0.02	0.02	0.02	0.03	0.03	0.02	0.03	0.03	0.03	0.02	0.03	0.03	0.02	0.03
Ca	0.01	0.00	0.00	0.00	0.00	0.00	0.00	0.00	0.00	0.01	0.00	0.00	0.00	0.00	0.01	0.00	0.00	0.00	0.00	0.00
Na	0.10	0.07	0.09	0.03	0.02	0.03	0.04	0.04	0.06	0.04	0.05	0.05	0.07	0.06	0.05	0.07	0.06	0.24	0.06	0.08
K	0.00	0.01	0.01	0.00	0.00	0.00	0.00	0.00	0.00	0.01	0.00	0.00	0.00	0.00	0.00	0.00	0.00	0.00	0.00	0.00
ΣChC	0.11	0.08	0.09	0.03	0.02	0.03	0.04	0.05	0.06	0.05	0.06	0.05	0.06	0.08	0.07	0.05	0.07	0.24	0.07	0.08
M	0.36	0.40	0.41	0.42	0.46	0.47	0.47	0.47	0.45	0.46	0.48	0.48	0.52	0.52	0.52	0.53	0.55	0.55	0.55	0.55

ΣChC and M are the sum of channel cations and Mg/(Mg+Mn+Fe) respectively.

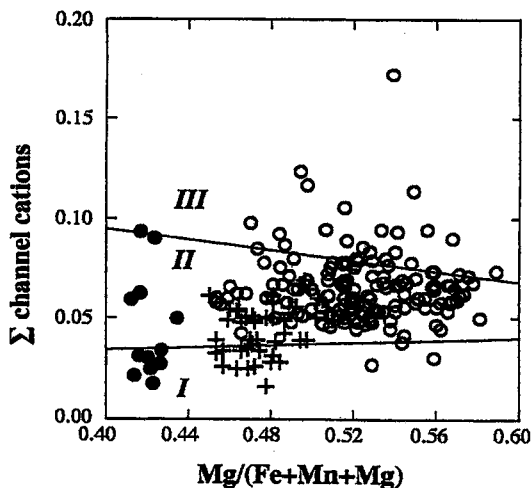


FIG. 4. Projection of compositions from each textural variety of cordierite in the Σ channel cations versus $Mg/(Mg+Fe+Mn)$ diagram. Symbols: black dots represent retrograde crystals, crosses, metamorphic crystals, and circles, magmatic crystals; I, II, and III represent fields of metamorphic, anatectic, and magmatic cordierites, respectively.

all crystals from types II and III seem magmatic. The relative importance of these compositional groups for each lithotype changes systematically from the less evolved migmatites to the most evolved anatectic leucogranites as follows: 1) The composition of cordierite in schlieren-type and nebulitic migmatites defines a bimodal distribution. Most cordierite crystals belong to the type Ia, and the rest to type II. 2) The composition of cordierite in transitional migmatites also is bimodal, with one mode corresponding to type Ib and the other to type II. In contrast to the above situation, type-II crystals are the more abundant. 3) The composition of cordierite in the subautochthonous granodiorite also is bimodal. One maximum corresponds to type II as in migmatites, but a new maximum appears. This is formed by type-III cordierite, which corresponds texturally to the largest magmatic-looking crystals. 4) Lastly, cordierite-bearing leucogranite also shows two maxima, but in this case with very different $Mg/(Mg+Fe+Mn)$ values. Type-III cordierite crystals are widespread, followed by those of type Ib.

Another important difference between type-II and type-III crystals lies in the patterns of zoning (Fig. 6). Type-II cordierite shows normal zoning, with $Mg/(Mg+Fe+Mn)$ decreasing from the core to the rim. In contrast, type-III crystals are inversely zoned, with $Mg/(Mg+Fe+Mn)$ increasing from the core to the rim

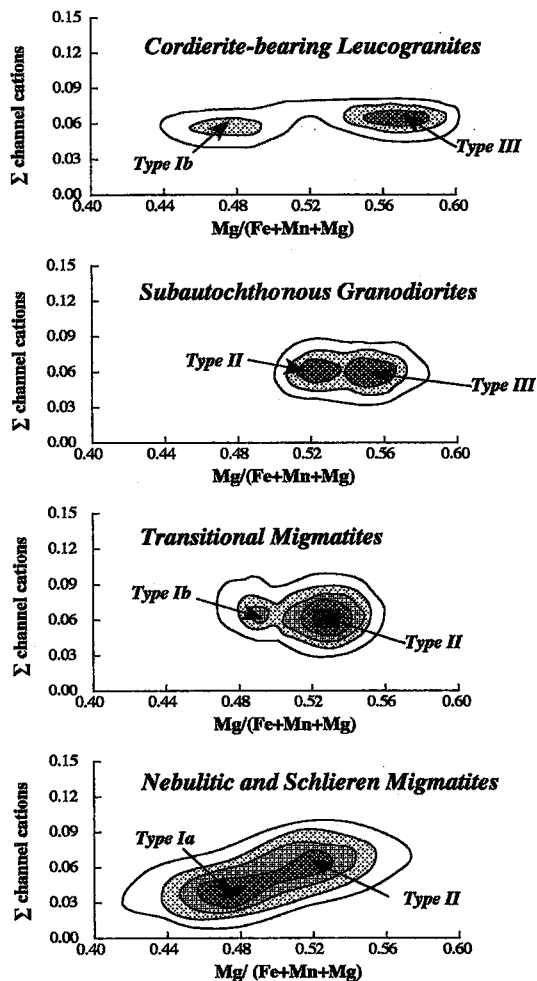


FIG. 5. Sample-density contour plots in the Σ channel cations versus $Mg/(Mg+Fe+Mn)$ diagram for each Peña Negra lithotype. Contours were estimated with the Epanechnikov kernel (Systat 1992)."

of crystals. This phenomenon of inverse zoning is very common in cordierite crystals of magmatic paragenesis, having been observed in experimental melts (Holtz & Johannes 1991) as well as in volcanic environments (e.g., Birch & Gleadow 1974).

Biotite

Biotite of the mesocratic migmatite is aluminous and ferrous (Table 4). Previous results of analyses by wet chemistry on concentrates (Bea 1980), together with the fact that the biotite usually is associated with

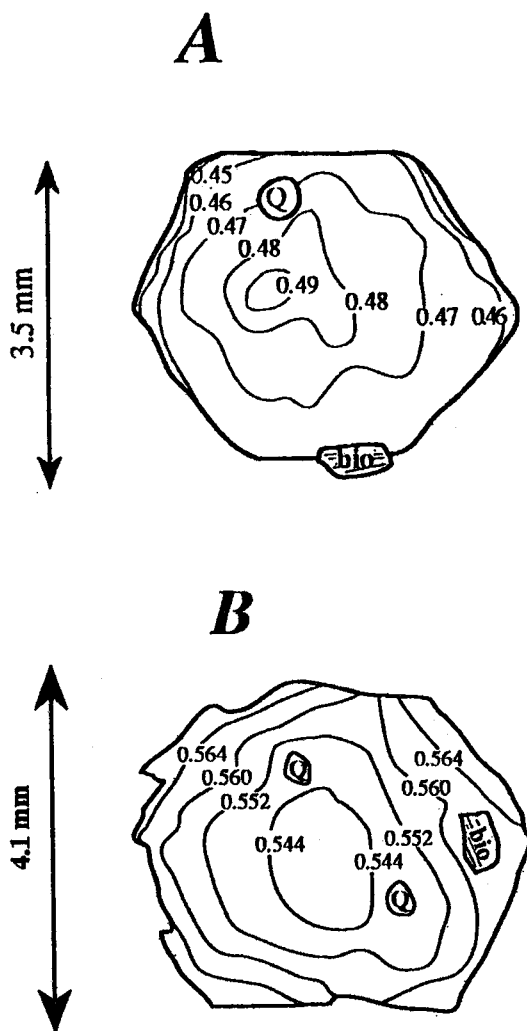


FIG. 6. Reverse $Mg/(Mg+Fe+Mn)$ zoning in magmatic crystals of cordierite. A. Type-II crystal from a mesocratic migmatite. B. Type-III crystal from a sample of sub-autochthonous granodiorite.

the ilmenite + sulfide + graphite, indicate that the amount of Fe^{3+} is very low (see Guidotti & Dyar 1991). The Ti contents range from moderate to high, with TiO_2 commonly in excess of 3 wt.%, and normally display a large variation among points analyzed in the same section. Averaged values for each section do not show any significant correlation with $Fe/(Fe+Mg)$

TABLE 4. RESULTS OF ELECTRON-MICROPROBE ANALYSIS AND STRUCTURAL FORMULA OF SELECTED CRYSTALS OF BIOTITE FROM PEÑA NEGRA LITHOTYPES

	Migmatites						Granodiorites						Leucogranites					
	1	2	3	4	5	6	7	8	9	10	11	12	13	14	15	16	17	18
Major element composition (wt. %)																		
SiO ₂	34.66	33.95	35.67	36.08	34.68	35.30	35.53	35.74	33.51	35.63	34.05	34.11	34.38	35.00	34.97	34.61	34.90	35.07
TiO ₂	2.96	3.33	2.09	2.74	3.06	3.20	3.17	3.35	3.32	2.97	3.17	2.69	2.97	1.95	3.95	2.56	2.67	2.93
Al ₂ O ₃	18.30	18.82	20.37	20.44	19.37	18.71	19.41	20.34	18.00	19.12	19.22	18.82	18.44	19.85	18.63	19.16	19.44	19.19
FeO	21.65	21.43	19.63	20.17	20.84	20.42	20.42	19.47	20.49	20.36	20.47	22.09	21.21	21.28	21.88	21.16	20.99	20.37
MgO	7.78	6.92	8.33	7.94	7.59	8.06	8.19	8.10	8.02	8.68	7.76	7.21	6.90	7.25	6.60	7.64	7.64	8.02
MnO	0.24	0.20	0.23	0.05	0.20	0.11	0.00	0.17	0.16	0.16	0.11	0.18	0.18	0.14	0.07	0.14	0.27	0.18
CaO	0.00	0.04	0.02	0.09	0.00	0.00	0.01	0.00	0.00	0.04	0.12	0.01	0.03	0.02	0.03	0.02	0.06	0.00
Na ₂ O	0.11	0.28	0.18	0.19	0.15	0.16	0.22	0.16	0.00	0.16	0.09	0.11	0.06	0.13	0.08	0.10	0.20	0.19
K ₂ O	9.79	9.32	9.35	8.88	9.56	9.16	9.46	9.48	9.64	9.44	9.40	9.26	9.14	8.93	9.20	8.72	9.14	9.37
Sum	95.49	94.29	95.87	96.58	95.45	95.12	96.41	96.81	93.14	96.56	94.39	94.48	93.31	94.55	95.41	94.11	95.31	95.32
Structural formula based on 11 oxygens																		
Si	2.68	2.65	2.69	2.70	2.66	2.70	2.68	2.67	2.65	2.69	2.64	2.66	2.70	2.70	2.69	2.68	2.68	2.68
^{IV} Al	1.32	1.35	1.31	1.30	1.34	1.30	1.32	1.33	1.35	1.31	1.36	1.34	1.30	1.30	1.31	1.32	1.32	1.32
^{VI} Al	0.34	0.38	0.51	0.50	0.41	0.39	0.41	0.46	0.32	0.39	0.40	0.39	0.41	0.51	0.38	0.44	0.43	0.41
Ti	0.17	0.20	0.12	0.15	0.18	0.18	0.18	0.19	0.20	0.17	0.18	0.16	0.18	0.11	0.23	0.15	0.15	0.17
Mg	0.90	0.81	0.94	0.88	0.87	0.92	0.92	0.90	0.94	0.98	0.90	0.84	0.81	0.83	0.76	0.88	0.87	0.91
Fe	1.40	1.40	1.24	1.26	1.34	1.31	1.29	1.22	1.35	1.28	1.33	1.44	1.39	1.37	1.41	1.37	1.35	1.30
Mn	0.02	0.01	0.01	0.00	0.01	0.01	0.00	0.01	0.01	0.01	0.01	0.01	0.01	0.01	0.00	0.01	0.02	0.01
Ca	0.00	0.00	0.00	0.01	0.00	0.00	0.00	0.00	0.00	0.00	0.01	0.00	0.00	0.00	0.00	0.00	0.00	0.00
Na	0.02	0.04	0.03	0.03	0.02	0.02	0.03	0.02	0.00	0.02	0.01	0.02	0.01	0.02	0.01	0.02	0.03	0.03
K	0.96	0.93	0.90	0.85	0.94	0.89	0.91	0.90	0.97	0.91	0.93	0.92	0.92	0.88	0.90	0.86	0.89	0.91
Fe/(Fe+Mg)	0.61	0.63	0.57	0.59	0.61	0.59	0.58	0.57	0.59	0.57	0.60	0.63	0.63	0.62	0.65	0.61	0.61	0.59

values (Fig. 7). However, results of individual analyses obtained on the same section reveal two types of correlation (Fig. 7): samples without modal garnet invariably show a positive correlation between Fe and Ti, whereas garnet-bearing samples invariably show a negative correlation.

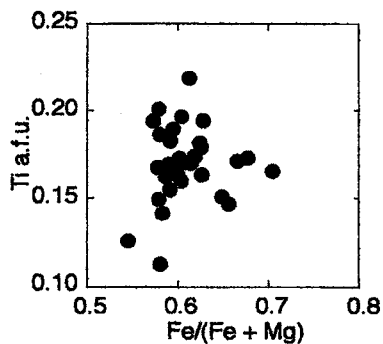
The composition of biotite crystals in the cordierite-bearing leucogranite is exactly the same as in mesocratic migmatite, which could be due to their restitic origin, as is clearly revealed by their textural relationships. However, the composition of biotite in the granodiorite differs markedly from that in the migmatite: 1) The frequency distribution of Fe/(Fe+Mg) values for biotite from mesocratic migmatites is not the same as for the subautochthonous granodiorite (Fig. 8), in spite of whole-rock Fe/(Fe+Mg) values being identical for both lithotypes. The frequency distribution is asymmetrical, ending sharply toward low values, and the mode is between a Fe/(Fe+Mg) value of 0.59 and 0.60. The frequency distribution of Fe/(Fe+Mg) for biotite from the subautochthonous granodiorite, however, is more symmetrical and incipiently bimodal, one mode at Fe/(Fe+Mg) in the range 0.57–0.58 and other, more intense, placed at a Fe/(Fe+Mg) value in the range 0.60–0.61. 2) The correlation between Ti and Fe/(Fe+Mg) is positive in

both the subautochthonous granodiorite and mesocratic migmatite. Nevertheless, ^{IV}Al and Fe/(Fe+Mg) are positively correlated in migmatite, but negatively so in granodiorite (Fig. 9).

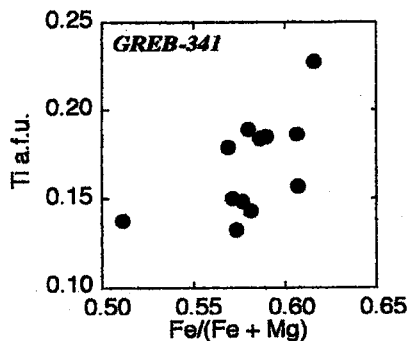
These differences in biotite and cordierite composition within each lithotype as well as from one lithotype to another obviously reflect different reactions involving biotite. These will be discussed below.

FIG. 7. Correlation between Ti (apfu) and Fe/(Fe+Mg) in biotite in mesocratic migmatite. A. Averaged values for each thin section. B. Sections with modal garnet. C. Sections without modal garnet. Though the average values show no correlation, note how data from individual sections are well correlated, those with modal garnet positively, and those without modal garnet negatively.

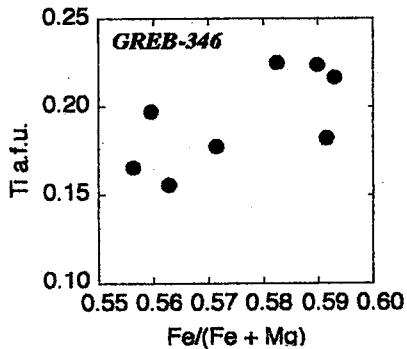
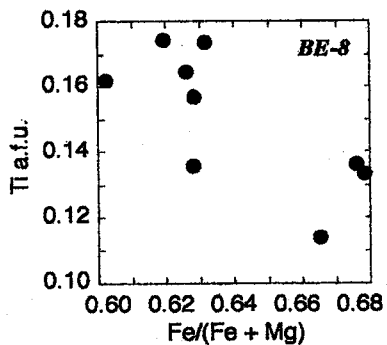
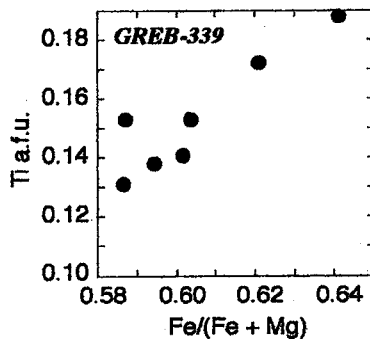
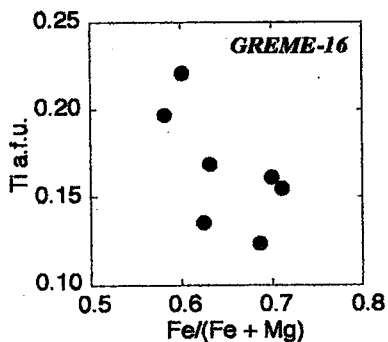
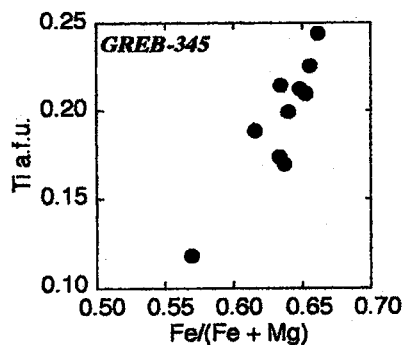
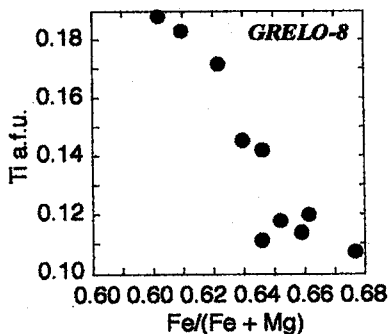
A



C



B



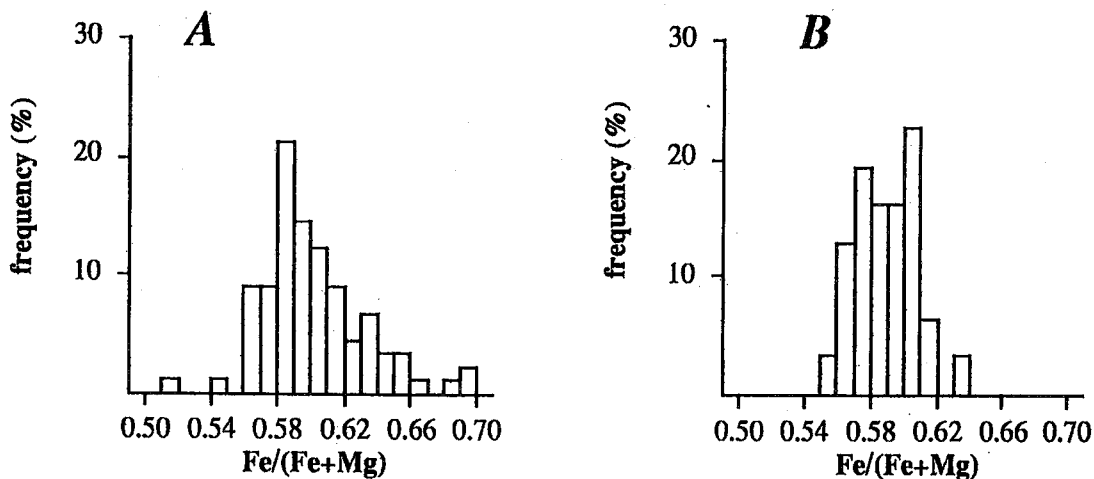


FIG. 8. Histogram of Fe/(Fe+Mg) values for biotite from mesocratic migmatite (A) and subautochthonous granodiorite (B). Note the bimodality of the latter, with the appearance of a new mode toward the magnesian side.

Garnet

The scarce crystals of garnet appear either in the leucosome or melanosome of the mesocratic migmatite, although the composition is exactly the same in both cases. In general, they consist of strongly zoned, spessartine-rich (up to 8 wt.% MnO) almandine-rich garnet with a Fe-, Mn-rich rim and a Mg-rich core (Table 5).

Sillimanite

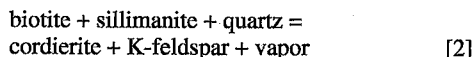
Sillimanite is slightly nonstoichiometric although, conversely to what has been described in the literature (Kerrick 1990), it has a moderate excess of Si and a corresponding coupled deficit of Al (Pereira 1992). Regarding other elements, sillimanite contains considerable amounts of Fe, although some crystals from restite also have high levels of Ti and Mn (Table 5).

Ilmenite

Ilmenite crystals have an almost stoichiometric composition, with some Mn substituting Fe. MnO is normally close to 2 wt.%, but in some specimens may rise to 5 wt.% (Table 5).

THE CORDIERITE-PRODUCING REACTIONS IN THE CASE OF THE METAMORPHIC CORDIERITE

The fact that biotite, sillimanite, and quartz never were found in contact within the melanosome of the mesocratic migmatite indicates that the neosome was formed according to the reaction:

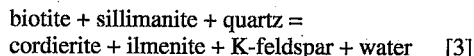


(e.g., Holdaway & Lee 1977).

Inasmuch as the Ti contents and Fe/(Fe+Mg) values are systematically higher in biotite than in coexisting cordierite, it is obvious that the formal expression of reaction [2] is a model that is too simple to correspond to mass balance in the real rocks. To satisfy mass balance, the reaction either has to be continuous with biotite on both sides of the equation, or a Ti-Fe-rich phase must appear as a reaction product together with cordierite and K-feldspar, or both.

The formation of ilmenite

The excess of Ti and Fe in biotite with respect to cordierite can be accommodated through the formation of ilmenite (e.g., Jamieson 1984; Bea 1989), such that equation [2] could be rewritten as follows:



The abundance of ilmenite in the melanosome and restite (Table 1) strongly supports this idea. However, attempts to calculate the mass balance using the real composition of minerals failed in all cases. As an example, we shall consider sample 3 (Table 2), a sample of typical mesocratic migmatite of schlieren type, with mostly type-Ia cordierite crystals. Using the numerical method developed by Bea (1989), the mass-balance adjustment of reaction [3] gives the following results:

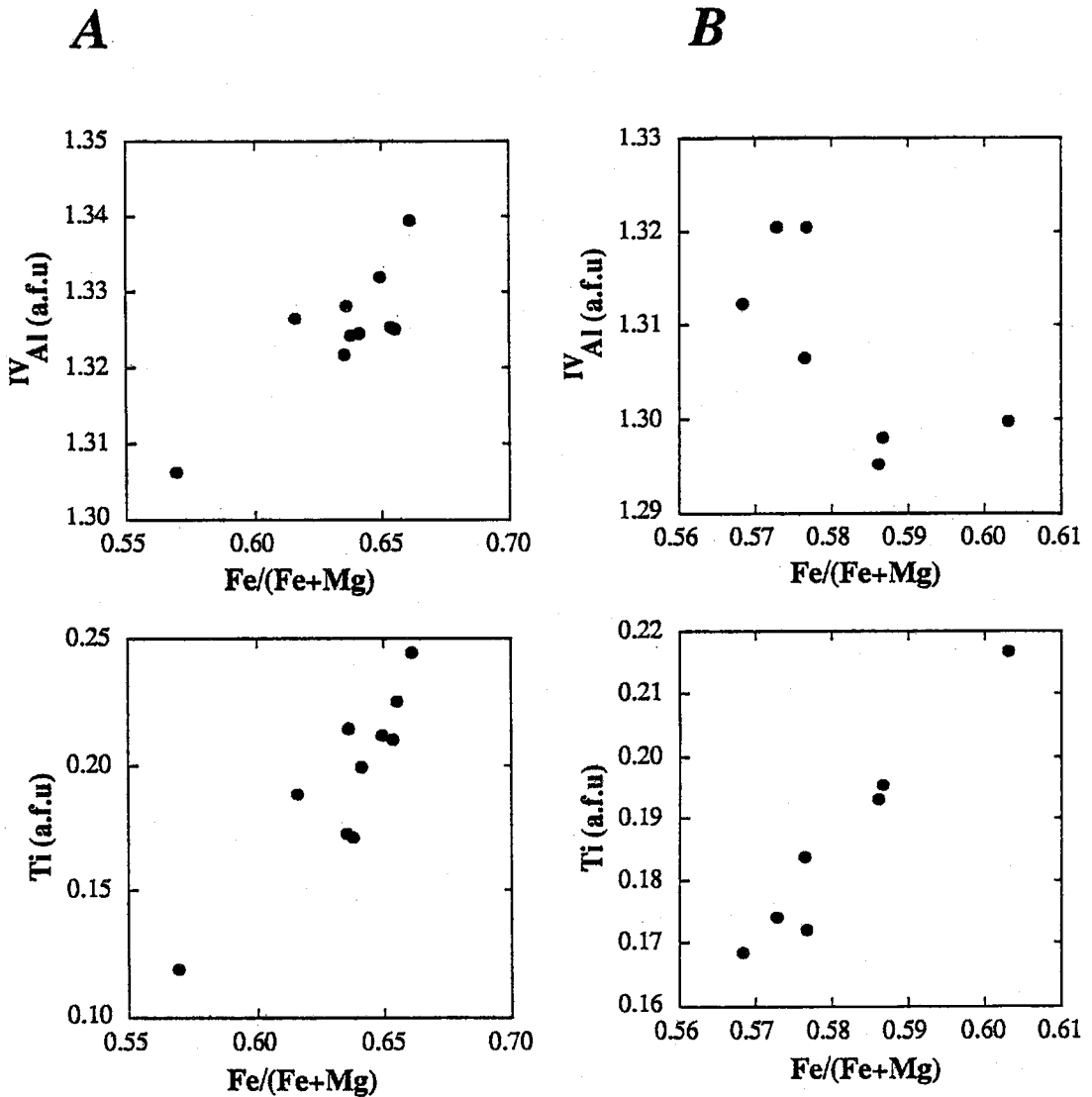
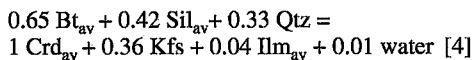


Fig. 9. Correlation between concentrations of Ti and ^{IV}Al (a.f.u) with Fe/(Fe+Mg) in biotite from two representative sections, one from mesocratic migmatite (A) and the other from subautochthonous granodiorite (B). Note how the correlation between ^{IV}Al and Fe/(Fe+Mg) shows opposite sign in both lithotypes, whereas the correlation between Ti and Fe/(Fe+Mg) is positive in both cases. See text for explanation.



However, this calculation has to be rejected, because it gives a high residual ($S^2 = 2.27$, where

$$S^2 = \sum_{i=\text{K}_2\text{O}}^{\text{SiO}_2} [\text{Crd}_i^{\text{calculated}} - \text{Crd}_i^{\text{measured}}]^2$$

and the theoretical composition of the cordierite produced is not realistic, with negative TiO_2 and an Fe/(Fe+Mg) ratio much higher than that of average cordierite (Table 6).

Continuous reaction with formation of biotite on both sides of the equation

Blümel & Schreyer (1977) suggested that reaction [2] could be rewritten as follows:

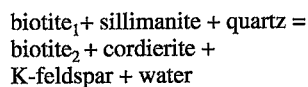


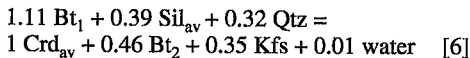
TABLE 5. RESULTS OF ELECTRON-MICROPROBE ANALYSIS AND STRUCTURAL FORMULA OF SELECTED SAMPLES OF GARNET, SILLIMANITE, AND ILMENITE FROM PEÑA NEGRA LITHOTYPES

	Garnet										Sillimanite				Ilmenite			
	1-1	1-2	1-3	1-4	1-5	2-1	2-2	2-3	2-4	2-5	1	2	3	4	1	2	3	4
Major element composition (wt. %)																		
SiO ₂	36.67	36.33	36.85	36.32	36.50	36.34	36.41	36.49	36.74	36.27	36.40	37.93	37.43	37.57	0.00	0.00	0.02	0.04
TiO ₂	0.04	0.05	0.02	0.03	0.02	0.02	0.02	0.83	0.00	0.07	0.05	0.00	0.01	0.03	53.45	53.36	52.46	52.55
Al ₂ O ₃	20.68	20.27	20.42	20.33	20.15	20.24	20.76	20.25	20.51	20.06	61.72	60.47	60.52	60.14	0.00	0.00	0.04	0.01
FeO	35.28	36.62	35.94	36.76	36.56	36.92	36.09	35.54	35.67	36.35	0.33	0.29	0.27	0.29	43.90	44.99	45.00	44.57
MgO	2.84	2.29	2.12	1.37	1.10	1.06	1.96	2.30	2.55	1.56	0.02	0.01	0.00	0.01	0.08	0.08	0.05	0.06
MnO	3.13	3.18	3.30	4.05	4.38	4.17	3.50	3.23	3.38	4.46	0.08	0.06	0.08	0.00	2.68	1.08	1.98	2.06
CaO	0.81	0.84	0.83	0.74	0.81	0.79	0.80	0.78	0.82	0.83	0.02	0.02	0.01	0.03	0.03	0.00	0.04	0.00
Na ₂ O	0.00	0.01	0.00	0.00	0.00	0.00	0.03	0.03	0.07	0.00	0.00	0.05	0.00	0.08	0.00	0.07	0.02	0.00
K ₂ O	0.00	0.00	0.00	0.00	0.00	0.00	0.00	0.00	0.00	0.00	0.00	0.00	0.00	0.00	0.00	0.00	0.00	0.10
Sum	99.44	99.59	99.48	99.59	99.51	99.55	99.56	99.45	99.73	99.60	98.62	98.83	98.32	98.15	100.14	99.58	99.61	99.39
Structural formula based on 12 (garnet), 5 (sillimanite) and 3 (ilmenite) oxygens																		
Si	2.99	2.98	3.01	2.99	3.01	3.00	2.98	2.98	3.00	2.99	1.00	1.04	1.03	1.03	0.00	0.00	0.00	0.00
Al	1.99	1.96	1.97	1.97	1.96	1.97	2.00	1.95	1.97	1.95	1.99	1.95	1.96	1.95	0.00	0.00	0.00	0.00
Ti	0.00	0.00	0.00	0.00	0.00	0.00	0.00	0.05	0.00	0.00	0.00	0.00	0.00	0.00	1.01	1.01	1.00	1.00
Fe	2.40	2.51	2.46	2.53	2.52	2.55	2.47	2.43	2.43	2.51	0.01	0.01	0.01	0.01	0.92	0.95	0.95	0.95
Mg	0.34	0.28	0.26	0.17	0.14	0.13	0.24	0.28	0.31	0.19	0.00	0.00	0.00	0.00	0.00	0.00	0.00	0.00
Mn	0.22	0.22	0.23	0.22	0.31	0.29	0.24	0.22	0.23	0.31	0.00	0.00	0.00	0.00	0.06	0.02	0.04	0.04
Ca	0.07	0.07	0.07	0.07	0.07	0.07	0.07	0.07	0.07	0.07	0.00	0.00	0.00	0.00	0.00	0.00	0.00	0.00
Na	0.00	0.00	0.00	0.00	0.00	0.00	0.00	0.00	0.01	0.00	0.00	0.00	0.00	0.00	0.00	0.00	0.00	0.00
K	0.00	0.00	0.00	0.00	0.00	0.00	0.00	0.00	0.00	0.00	0.00	0.00	0.00	0.00	0.00	0.00	0.00	0.00

Analyses obtained by wavelength dispersive analyses with a CAMECA electron microprobe using synthetic standards. In both cases accelerating voltage was 15 kV and sample current was 10 nA.

Analyses from 1-1 (center) to 1-5 (border) belong to a single garnet crystal. Analyses from 2-1 (border) to 2-5 are a profile across another crystal of garnet. All sillimanite and ilmenite data are from mesocratic migmatites.

where biotite₁ represents a Ti-poor, low-Fe/(Fe+Mg) biotite, and biotite₂ is a higher-Fe/(Fe+Mg) biotite richer in Ti. This reaction has found support in the experimental work carried out by Le Breton & Thompson (1988) and Holtz & Johannes (1991), who described how biotite resulting from melting experiments are richer in Ti than biotite in the starting material. Since the compositional spectrum of the biotite from the mesocratic migmatite ranges, precisely, from individuals with low Ti and Fe/(Fe+Mg) up to others with high Ti and Fe/(Fe+Mg) (Fig. 7), equation [5] could well represent the situation in the Peña Negra Complex. The mass-balance adjustment gives the following results:

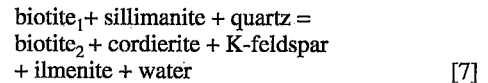


This equation has a better fit than before ($S^2 = 0.22$), but the theoretical composition of the cordierite is unacceptably high in Ti (Table 6). In addition, the equation does not explain the high contents of ilmenite in the Peña Negra migmatite, especially in restite and melanosome assemblages.

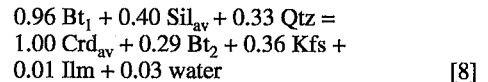
The combination of both mechanisms

It therefore seems reasonable to combine equations

[3] and [4] as follows:



Calculation of the stoichiometric coefficients of this equation gives:



with a very low residual ($S^2 = 0.03$) and a theoretical composition of cordierite (Table 6) that almost exactly

TABLE 6. MAJOR-ELEMENT COMPOSITION OF MINERALS FROM SAMPLE 3 USED IN MASS-BALANCE CALCULATIONS OF EQUATIONS [4], [6] AND [8]

	Bt ₁	Bt ₂	B _{av}	Sil _{av}	Ilm _{av}	Crd _{av}	Crd _[4]	Crd _[6]	Crd _[8]
SiO ₂	35.67	34.67	35.12	36.98	0.00	47.89	47.89	47.89	47.89
TiO ₂	2.09	4.23	3.10	0.01	54.30	0.01	-0.37	0.38	0.03
Al ₂ O ₃	20.37	18.45	19.51	62.02	0.00	32.19	32.19	32.19	32.19
FeO	19.63	22.69	21.48	0.37	43.04	11.69	12.20	11.56	11.68
MgO	8.33	6.55	7.27	0.03	0.00	6.05	4.73	6.27	6.06
MnO	0.23	0.14	0.14	0.01	2.20	0.33	0.00	0.20	0.15
CaO	0.01	0.01	0.01	0.00	0.00	0.01	0.01	0.01	0.01
Na ₂ O	0.18	0.09	0.11	0.02	0.00	0.18	0.08	0.17	0.16
K ₂ O	9.35	9.57	9.44	0.00	0.00	0.01	0.01	0.01	0.01

Crd_[4], Crd_[6], and Crd_[8] are the theoretical composition of cordierite obtained through these equations. Composition is given in wt. %

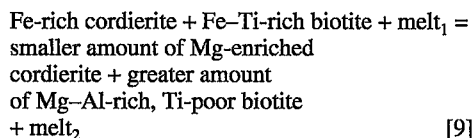
matches the average value of real cordierite and can therefore be accepted as representing the real situation responsible for type-Ia cordierite.

Type-Ib crystals, on the other hand, only differ from those of type Ia in the higher ΣChC contents in the former. Type-Ib crystals could originate either by reaction of previous type-Ia crystals with the melt, or directly by reaction [8] if it occurred after the beginning of partial melting.

THE CORDIERITE-PRODUCING REACTIONS IN THE CASE OF THE MAGMATIC CORDIERITE

Experimental work by Holtz & Johannes (1991) on materials very similar to the Peña Negra migmatites has revealed that: (1) cordierite in contact with the melt occurs as idiomorphic crystals, (2) these are invariably inversely zoned, and (3) the Mg content of the rim increases with both temperature (at constant pressure and melt fraction) and with the melt fraction (at constant pressure and temperature). These findings are in excellent agreement with the changes described above in the composition of magmatic cordierite, from low-Mg, normally zoned crystals (type II) in the leucosome of migmatites, up to high-Mg, inversely zoned crystals (type III) in the granitic rocks. The latter, therefore, seem to be the result of the increase in the degree of partial melting and the effectiveness of the separation between melt and restite. To determine which mineral reactions may be involved in such a process, the restite-rich, high-melt-fraction sub-autochthonous granodiorite will be examined more closely.

The modal abundance of cordierite decreases from migmatite to granodiorite but, at the same time, crystals become larger and more idiomorphic. This may indicate the existence of the Ostwald ripening effect, in which small crystals are dissolved in the melt, whereas larger ones grow. However, this effect alone cannot explain why the growing crystals become progressively more magnesian, and we must look for a reaction with the other ferromagnesian mineral present in the system, *i.e.*, biotite. Note that the biotite from granodiorite, as opposed to that from migmatite, simultaneously displays a negative correlation of ^{IV}Al versus $\text{Fe}/(\text{Fe}+\text{Mg})$ and a positive correlation of Ti versus $\text{Fe}/(\text{Fe}+\text{Mg})$. This reveals that they were involved in a continuous reaction that produced less Ti-rich but more Mg- and Al-rich biotite, exactly what one would expect from the destruction of a Ti-poor, Mg-Al-rich phase such as cordierite. This reaction could be summarized as follows:

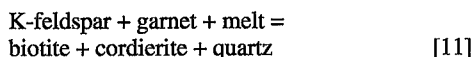
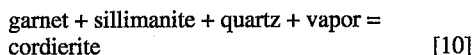


The net amount of biotite increases, but that of cordierite decreases to the right. Unfortunately, lack of accurate knowledge of the composition of the melt prevents any mass-balance calculations.

The origin of cordierite in leucogranite also can be understood through a mechanism similar to that described in [9]. These leucogranitic rocks have low whole-rock $\text{Fe}/(\text{Fe}+\text{Mg})$ values, in some cases even lower than in the mesocratic migmatite (Pereira 1992). Considered together with the fact that biotite is less abundant than cordierite, this finding strongly supports the idea that cordierite dissolved easily in the melt, whereas biotite did not.

CORDIERITE-PRODUCING RETROGRADE REACTIONS

Cordierite grains that surround garnet crystals have high Mn contents and $\text{Fe}/(\text{Fe}+\text{Mg})$ ratios, in sharp contrast to other cordierite crystals in the same thin section. The crystals of biotite around garnet also are less magnesian than average biotite within the same thin section, but in this case differences are more subtle than for cordierite (Fig. 9). On the other hand, garnet crystals always show a pattern of inverse zoning consistent with a long history of re-equilibration and cooling, from T and P approximately 780–800°C and 4–4.3 kbar down to 450°C and 1.5 kbar (Pereira 1992, 1993). These facts are consistent with the retrogression of garnet through a reaction in which biotite and cordierite grew from garnet. As a first approach, two extreme cases could be considered:



(*e.g.*, Thompson 1982, Grant 1985a), with reaction [10] being relatively insensitive to temperature, and [11] relatively insensitive to pressure.

Equation 11 cannot be balanced without the composition of the melt (see Grant 1993). Besides, the following evidence militates against this reaction: there is no quartz around the grains of garnet, the amount of biotite is always subordinate to that of cordierite, and the reaction continued at temperatures far below the liquidus. Therefore, it can be disregarded.

The mass balance in equation [10] cannot be adjusted unless other minerals also participate. Both the negative correlation between Ti and $\text{Fe}/(\text{Fe}+\text{Mg})$ in biotite and the retrograde zoning in garnet suggest that the reaction was a continuous one, with biotite and garnet on both sides of the equation. After computing different possibilities using the composition of minerals given in Table 7, the best mass-balance equation was found to be:

TABLE 7. MAJOR-ELEMENT COMPOSITION OF MINERALS FROM SAMPLE 3 (TABLE 2) USED IN MASS-BALANCE CALCULATION FOR EQUATION [12]

	Bt ₁	Bt ₂	Sil _{av}	Grt ₁	Grt ₂	Ilm _{av}	Crd _{av}
SiO ₂	34.49	34.27	37.96	36.25	36.23	0.00	47.39
TiO ₂	3.27	1.84	0.02	0.04	0.00	54.28	0.01
Al ₂ O ₃	19.16	20.00	62.36	20.51	20.77	0.00	32.19
FeO	20.72	23.22	0.33	33.99	34.29	42.14	12.12
MgO	7.40	6.19	0.03	2.80	0.61	0.00	5.29
MnO	0.12	0.15	0.02	3.52	5.59	4.12	0.55
CaO	0.01	0.20	0.01	0.76	0.69	0.00	0.10
Na ₂ O	0.28	0.37	0.01	0.00	0.09	0.00	0.46
K ₂ O	9.20	8.72	0.02	0.01	0.02	0.00	0.00

Composition is given in wt.%

$$\begin{aligned}
 &2.13 \text{ Bt}_1 + 1.38 \text{ Grt}_1 + 0.35 \text{ Sil} + \\
 &0.09 \text{ Qtz} + 0.09 \text{ Ab (from plagioclase)} = \\
 &1 \text{ Crd}_{\text{av}} + 2.25 \text{ Bt}_2 + 0.72 \text{ Grt}_2 + 0.05 \text{ Ilm} + \\
 &0.001 \text{ An (to plagioclase)} \quad [12]
 \end{aligned}$$

which gives a null residual ($S^2 = 0$) and a theoretical composition of biotite exactly equal to that targeted in the model. This equation involves the creation of 1 g of cordierite plus 0.12 g of biotite from 0.66 g of garnet plus 0.35 g of sillimanite, which is consistent with textural observations.

THE ROLE OF CORDIERITE DURING ANATEXIS

Experimental work by Schairer (1954) and Seifert (1976) has revealed that at low pressure, the assemblage quartz + K-feldspar + cordierite + vapor in the KFMASH system melts congruently at a temperature several tens of degrees below the quartz + K-feldspar + vapor = L solidus. Grant & Hoffer (1977) and Grant (1985a, b) also have shown that in the KFMASH system, a low-temperature field of liquid extends at least to intermediate Fe/(Fe+Mg) values owing to the congruent melting of the assemblage quartz + K-feldspar + cordierite + vapor. The mineralogy of the almost pure-melt cordierite-bearing leucogranitic rocks, rich in quartz and K-feldspar, with magmatic cordierite as the dominant ferromagnesian phase, strongly supports the hypothesis that melting could have started in this way.

To evaluate the influence of small differences in the P-T path on the amount and composition of the melt generated anatexically, we once again focus on sample 3 (Table 2). Let us suppose that two rocks, α and β , having the chemical composition of sample 3, evolve following two different P-T paths (A and B, respectively), one at lower pressure than the other (Fig. 10). At 600–650°C, the mineral assemblage in both rocks will be different because rock α , following the low-P path A, intersects the univariant reaction modeled by equation [2], and thus has cordierite + K-feldspar stable, whereas rock β has biotite + sillimanite + quartz stable. The modal composition of rock

α should be the same as the actual composition of sample 3, and the composition of rock β can easily be calculated from equation [8] (Table 8). Taking these differences into account, the following arguments clearly indicate that the rock evolving along the lower-P path will yield a greater proportion of melt.

Rock α , equilibrated at lower pressure, has a higher modal percentage of quartz + feldspars. It is thus more fertile than rock β if anatexis takes place at temperatures somewhere within the interval between the water-saturated haplogranite solidus ($\sim 650^\circ\text{C}$ at 3.5 kbar, Johannes & Holtz 1990) and the incongruent melting of biotite ($\sim 760^\circ\text{C}$ at 3.5 kbar under vapor-absent conditions: Vielzeuf & Holloway 1988, Le Breton & Thompson 1988, Patiño Douce & Johnston 1991). Another factor that increases the relative fertility of rock α is that at the intersection with the H₂O-saturated granite solidus, rock α has more water available for melting, owing to the destruction of biotite to give cordierite. A simple mass-balance calculation, assuming that all water available in rock β comes from the breakdown of muscovite to give sillimanite plus K-feldspar, leads an estimate of about 0.8 and 0.4 wt.% of H₂O for rocks α and β . Application of diagrams of melt productivity in fluid-absent conditions (e.g., Clemens & Vielzeuf 1987, Johannes & Holtz 1990) suggests melt fractions of 0.15 for rock α and 0.05 for rock β , respectively. Lastly, the above-mentioned congruent melting of cordierite in the presence of K-feldspar, quartz, and water at temperatures below or the same as the haplogranite solidus must also contribute to the fact that, other conditions being equal, the melt fraction in rocks with modal cordierite is greater than in those with sillimanite + biotite.

Tracy & Robinson (1983) and Tracy (1985) have already interpreted the two styles of migmatization in central Massachusetts as being the consequence of different P-T paths. Low-melt-fraction stromatic migmatites were produced along a higher-pressure path, where only the vapor-absent melting curve of

TABLE 8. CALCULATED MODAL COMPOSITION OF TWO ROCKS, α AND β , WITH THE SAME CHEMICAL COMPOSITION AS SAMPLE 3 (TABLE 2), AS A RESULT OF DIFFERENT P-T PATHS AND EQUILIBRATED AT 600–750°C

	Modal composition of rock α	Coefficients of equation [8]	Amounts of mineral originated	Modal composition of rock β
Qtz	22.4	0.3263	4.1	26.5
Kfs	16.4	-0.3622	-4.5	11.9
Pl (An ₂₂)	31.2			31.2
Crd	12.6	-1.0000	-12.6	0.0
Bt	15.6	0.6634	8.3	23.9
Sil	0.8	0.3989	5.0	5.8
Ilm	0.4	-0.0140	-0.2	0.2
Others	0.4			0.4

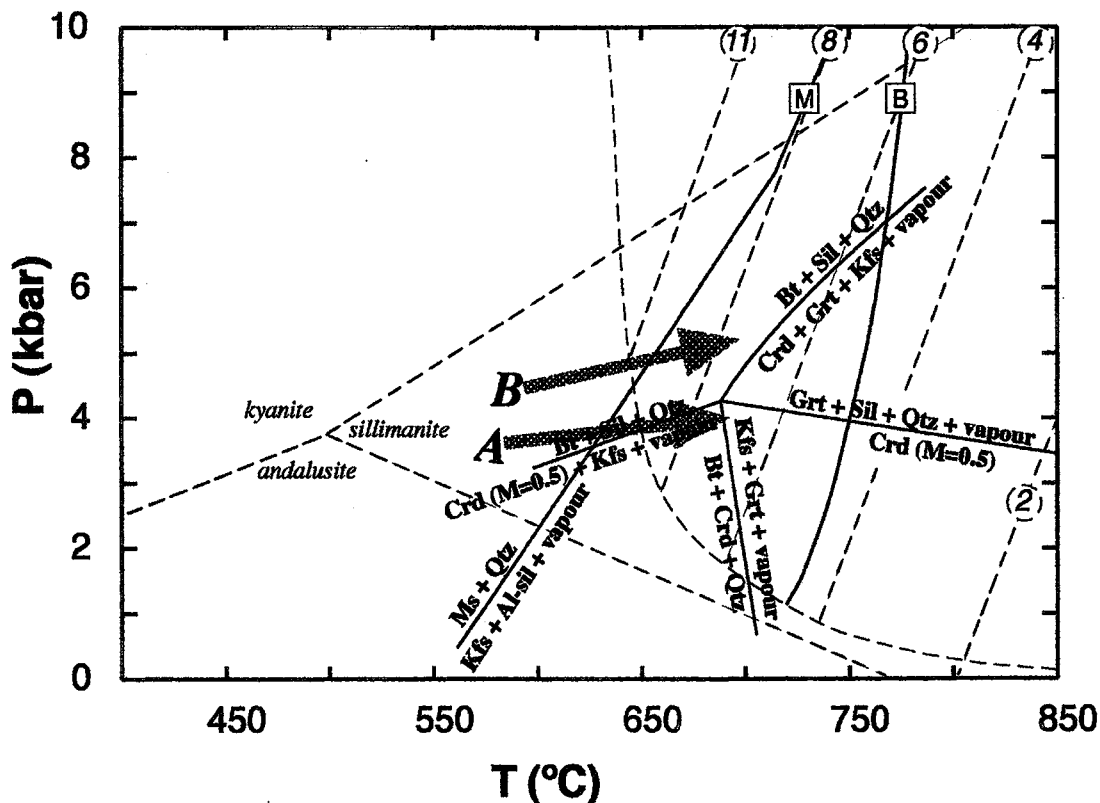
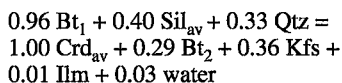


FIG. 10. High-fertility (A) and low-fertility (B) trends in low-pressure anatexis. See text for explanation. M curve, vapor-absent melting of muscovite [Chatterjee & Johannes (1974), as modified by Holdaway & Lee (1977)]. B curve: vapor-absent melting of biotite (Le Breton & Thompson 1988). Other univariant curves according to Holdaway & Lee (1977). Solidus curves for the haplogranitic system according to Johannes & Holtz (1990); numbers within circles are the percentage of water.

muscovite was crossed. Nebulitic migmatites, with a higher melt-fraction, on the other hand, were interpreted to develop along a lower-pressure path that crossed the vapor-absent melting curve of both micas, first muscovite and then biotite (see also Le Breton & Thompson 1988). Our observations fully agree with these ideas, but we also emphasize that it is not necessary to intersect the melting curve of biotite, as it is sufficient to intersect the univariant biotite + sillimanite + quartz = cordierite + K-feldspar + vapor below the haplogranite solidus.

CONCLUSIONS

During the prograde evolution of Peña Negra anatexites, cordierite first originated at subsolidus conditions through the continuous reaction:



which involved low-Ti, low-Fe/(Fe+Mg) biotite as a reactant, and high-Ti, high-Fe/(Fe+Mg) biotite and ilmenite as reaction products. The cordierite crystals thus formed are metamorphic and belong to the Ia compositional type, which is characterized by Mg/(Mg+Fe+Mn) less than 0.49 and ΣChC approximately equal to 0.035.

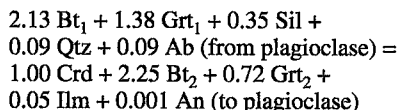
Type-Ib crystals have the same metamorphic appearance and Mg/(Mg+Fe+Mn) as those of type Ia, and differ only in their high content of channel cations ($\Sigma\text{ChC} \approx 0.60$). They originated either from the reaction of type-Ia crystals with the melt, or directly through the above reaction after the P-T path intercepted the haplogranite solidus.

Type-II crystals, magmatic, Mg/(Mg+Fe+Mn) in the range 0.51–0.53, normally zoned, also were produced by the same reaction, but at a melt fraction high enough so as not to constraint the geometry of growing crystals. The Mg/(Mg+Fe+Mn) values increase as the melt fraction increases, either due to the increase in temperature or water content or both.

Type-III crystals, magmatic, Mg/(Mg+Fe+Mn) greater than 0.51, inversely zoned, grew from the melt either by nucleating over old type-II or type-I crystals or from new nuclei. The first case probably represents the situation in the restite-rich, high-melt-fraction sub-autochthonous granodiorite, whereas the second one seems more widespread in the restite-poor, low-melt-fraction leucogranite. A continuous reaction between the melt and restitic biotite (before or after melt segregation) means that newly precipitated cordierite becomes progressively less abundant and more magnesian.

There is no discontinuity among these processes, as they are the result of the advancing anatectic evolution.

Retrograde cordierite was formed from garnet crystals through the continuous reaction:



which involved high-Ti, low-Fe(Fe+Mg) biotite and low-Mn garnet to give low-Ti, high-Fe/(Fe+Mg) biotite and high-Mn garnet.

P-T paths have a great influence on melt productivity. Within the temperature range 660–750°C, those rocks evolving along a lower-pressure path and then intercepting the invariant biotite + sillimanite + quartz = cordierite + K-feldspar + water at subsolidus conditions are more fertile than those evolving at higher pressure, although chemical composition could be the same.

The presence of cordierite in source rocks increases their fertility in two ways: (1) indirectly, because cordierite-producing reactions release water and K-feldspar, thus increasing the percentage of haplogranitic component in the anatectic system, and (2) directly, owing to congruent melting at low temperature in the presence of quartz and K-feldspar.

ACKNOWLEDGEMENTS

The authors are indebted to W. Johannes, L.S. Hollister, R.F. Martin, J.A. Grant and an anonymous referee whose comments greatly helped to improve the manuscript. Thanks are also given to F. Sassi and the Centro di Studi per i Problemi dell'Orogeno delle Alpi Orientali (C.N.R., Padova, Italy), for allowing the extensive use of their electron-microprobe facility, and to R. Carampin, for his assistance with the electron microprobe. This work has been supported by the CICYT grants GEO89-0600-CO3-01 and AMB93-0535, Spanish Ministry of Education.

REFERENCES

- ASHWORTH, J.R. & CHINNER, G.A. (1978): Coexisting garnet and cordierite in migmatites from the Scottish Caledonides. *Contrib. Mineral. Petrol.* **65**, 379-394.
- BEA, F. (1980): Geochemistry of biotites in an assimilation process. An approach to recognition of metamorphic biotites from magmatic occurrence. *Kristalinikum* **15**, 103-124.
- (1982): Sobre el significado de la cordierita en los granitoides del batolito de Avila (Sistema Central Español). *Bol. Geol. Min. España* **93-1**, 59-69.
- (1989): A method for modelling mass-balance in partial melting and anatectic leucosome segregation. *J. Metamorphic Geol.* **7**, 619-628.
- (1991): Geochemical modelling of low melt-fraction anatexis in a peraluminous system: the Peña Negra Complex (central Spain). *Geochim. Cosmochim. Acta* **55**, 1859-1874.
- & PEREIRA, M.D. (1990): Estudio petrológico del Complejo Anatóctico de la Peña Negra, Batolito de Avila. *Rev. Soc. Geol. España* **3**, 87-104.
- BIRCH, W.D. & GLEADOW, A.J.W. (1974): The genesis of garnet and cordierite in acid volcanic rocks: evidence from Cerberean Cauldron, central Victoria, Australia. *Contrib. Mineral. Petrol.* **45**, 1-13.
- BLÜMEL, P. & SCHREYER, W. (1977): Phase relations in pelitic and psammitic gneisses of the sillimanite - potash feldspar and cordierite - potash feldspar zones in the Moldanubicum of the Lam - Bodenmais area, Bavaria. *J. Petrol.* **18**, 431-459.
- BROWN, M. (1983): The petrogenesis of some migmatites from the Presqu'île de Rhuys, southern Brittany, France. In *Migmatites, Melting and Metamorphism* (M.P. Atherton & C.D. Gribble, eds.). Shiva Geology Series, Nantwich, Cheshire, U.K. (174-200).
- CHATTERJEE, N.D. & JOHANNES, W. (1974): Thermal stability and standard thermodynamic properties of synthetic $2M_1$ -muscovite $KAl_2(AlSi_3O_{10}(OH)_2)$. *Contrib. Mineral. Petrol.* **48**, 89-114.
- CLEMENS, J.D. & VIELZEUF, D. (1987): Constraints on melting and magma production in the crust. *Earth Planet. Sci. Lett.* **86**, 287-306.
- FITZSIMONS, I.C.W. & HARLEY S.L. (1991): Geological relationships in high-grade gneiss of the Brastrand Bluffs coastline, Prydz Bay, east Antarctica. *Aust. J. Earth Sci.* **38**, 497-519.
- GERVILLA, F. (1990): *Mineralizaciones magmáticas ligadas a la evolución de rocas ultramáficas de la Serranía de Ronda (Málaga - España)*. Tesis, Univ. Granada, Granada, Spain.

- GOLDMAN, D.S., ROSSMAN, G.R. & DOLLASE, W.A. (1977): Channel constituents in cordierite. *Am. Mineral.* **62**, 1144-1157.
- GRANT, J.A. (1985a): Phase equilibria in partial melting of pelitic rocks. In *Migmatites* (J.R. Ashworth, ed.), Blackie, Glasgow, U.K. (86-144).
- _____ (1985b): Phase equilibria in low-pressure partial melting of pelitic rocks. *Am. J. Sci.* **285**, 409-435.
- _____ (1993): Experimental melting of the natural assemblage quartz - K feldspar - biotite - cordierite from the Laramie Aureole, Morton Pass, Wyoming. *Geol. Soc. Am., Abstr. Programs* **25**(6), A-447.
- _____ & HOFFER, E. (1977): Reactions in pelitic migmatites in the light of hydrothermal melting experiments involving Mg-Fe cordierite. *Geol. Soc. Am., Abstr. Programs* **9**, 994.
- GUIDOTTI, C.V. & DYAR, M.D. (1991): Ferric iron in metamorphic biotite and its petrologic and crystallochemical implications. *Am. Mineral.* **76**, 161-175.
- HOLDAWAY, M.J. & LEE, S.M. (1977): Fe-Mg cordierite stability in high-grade pelitic rocks based on experimental, theoretical, and natural observations. *Contrib. Mineral. Petrol.* **63**, 175-198.
- HOLTZ, F. (1989): Importance of melt fraction and source rock composition in crustal genesis - the example of two granitic suites of northern Portugal. *Lithos*, **24**, 21-35.
- _____ & JOHANNES, W. (1991): Genesis of peraluminous granites. I. Experimental investigation of melt compositions at 3 and 5 kbar and various H₂O activities. *J. Petrol.* **32**, 935-958.
- IBARGUCHI, J.I.G. & MARTINEZ, F.J. (1982): Petrology of garnet - cordierite - sillimanite gneisses from El Tormes thermal dome, Iberian Hercynian Fold Belt (W Spain). *Contrib. Mineral. Petrol.* **80**, 14-24.
- JAMIESON, R.A. (1984): Low pressure cordierite-bearing migmatites from Kelly's Mountain, Nova Scotia. *Contrib. Mineral. Petrol.* **86**, 309-320.
- JOHANNES, W. & HOLTZ, F. (1990): Formation and composition of H₂O-undersaturated granitic melts. In *High-T Metamorphism and Crustal Anatexis* (J.R. Ashworth & M. Brown, eds.). Unwin Hyman, London.
- KERRICK, D.M. (1990): The Al₂SiO₅ polymorphs. *Rev. Mineral.* **22**.
- LEAKE, B.E. (1960): Compilation of chemical analyses and physical constants of natural cordierites. *Am. Mineral.* **45**, 282-298.
- LE BRETON, N. & THOMPSON, A.B. (1988): Fluid-absent (dehydration) melting of biotite in metapelites in the early stages of crustal anatexis. *Contrib. Mineral. Petrol.* **99**, 226-237.
- LEPEZIN, G.G., KZUNETZKOVA, I.K., LAVRENT'EV, YU.G. & CHMEL'NICOVA, O.S. (1976): Optical methods of determination of water contents in cordierites. *Contrib. Mineral. Petrol.* **58**, 319-329.
- PATIÑO DOUCE, A.E. & JOHNSTON, A.D. (1991): Phase equilibria and melt productivity in the pelitic system: implications for the origin of peraluminous granitoids and aluminous granulites. *Contrib. Mineral. Petrol.* **107**, 202-218.
- PEREIRA, M.D. (1989): *Migmatización diatexitica y la génesis de las granodioritas subautóctonas del Complejo Anatético de la Peña Negra, Batolito de Avila*. Tesis de Licenciatura, Univ. Salamanca, Salamanca, Spain.
- _____ (1992): *El Complejo Anatético de la Peña Negra (Batolito de Avila): un estudio de la anatexia cortical en condiciones de baja presión*. Tesis, Univ. Salamanca, Salamanca, Spain.
- _____ (1993): Geotermobarometría del granate en el Complejo de la Peña Negra, España central. Implicaciones sobre la evolución del metamorfismo hercínico. *Rev. Soc. Geol. España*, **6** (1-2), 131-140.
- _____ , RONKIN, Y. & BEA, F. (1992): Dataciones Rb/Sr en el Complejo Anatético de la Peña Negra (Batolito de Avila, España Central): Evidencias de magmatismo prehercínico. *Rev. Soc. Geol. España* **5**(1-2), 129-134.
- PERREAULT, S. & MARTIGNOLE, J. (1988): High-temperature cordierite migmatites in the north-eastern Grenville Province. *J. Metamorphic Geol.* **6**, 673-696.
- ROTTURA, A., BARGOSI, G.M., CAIRONI, V., D'AMICO, C. & MACCARRONE, E. (1989): Petrology and geochemistry of late-hercynian granites from the western Central System of the Iberian Massif. *Eur. J. Mineral.* **1**, 667-683.
- SCHAIRER, J.F. (1954): The system K₂O-MgO-Al₂O₃-SiO₂. *J. Am. Ceram. Soc.* **37**, 501-533.
- SCHREYER, W. (1965): Synthetische und natürliche Cordierite. II. Die chemischen Zusammensetzungen natürlicher Cordierite und ihre Abhängigkeit von den PTX-Bedingungen bei der Gesteinsbildung. *Neues Jahrb. Mineral. Abh.* **103**, 35-79.
- _____ , MARESH, W.V., DANIELS, P. & WOLFSORFF, P. (1990): Potassic cordierites: characteristic minerals for high-temperature, very low-pressure environments. *Contrib. Mineral. Petrol.* **105**, 162-172.
- SECCHI, F.A., BROTZU, P. & CALLEGARI, E. (1991): The Arburese igneous complex (SW Sardinia, Italy) - an example of dominant igneous fractionation leading to peraluminous cordierite-bearing leucogranites as residual melts. *Chem. Geol.* **92**, 213-249.
- SEIFERT, F. (1976): Stability of the assemblage cordierite + K feldspar + quartz. *Contrib. Mineral. Petrol.* **57**, 179-185.

- SPEER, J.A. (1981): Petrology of cordierite- and almandine-bearing granitoid plutons of the Southern Appalachian Piedmont, U.S.A. *Can. Mineral.* **19**, 35-46.
- SYSTAT, Inc. (1992). *Graphics. Version 5.2 Edition.* Evanston, Ill.
- THOMPSON, A.B. (1982): Dehydration melting of pelitic rocks and the generation of H₂O-undersaturated granitic liquids. *Am. J. Sci.* **282**, 1567-1595.
- TRACY, R.J. (1985): Migmatite occurrences in New England. In *Migmatites, Melting and Metamorphism* (M.P. Atherton & C.D. Gribble, eds.). Blackie, Glasgow, U.K. (204-224).
- _____ & ROBINSON, P. (1983): Acadian migmatite types in pelitic rocks of central Massachusetts. In *Migmatites, Melting and Metamorphism* (M.P. Atherton & C.D. Gribble, eds.). Shiva Geology Series, Nantwich, Cheshire, U.K. (163-173).
- VERNON, R.H., CLARKE, G.L. & COLLINS, W.J. (1990): Local, mid-crustal granulite facies metamorphism and melting: an example in the Mount Stafford area, central Australia. In *High-Temperature Metamorphism and Crustal Anatexis* (J.R. Ashworth & M. Brown, eds.). Unwin Hyman, London, U.K. (272-319).
- VIELZEUF, D. & HOLLOWAY, J.R. (1988): Experimental determination of the fluid-absent melting relations in the pelitic system. Consequences for crustal differentiation. *Contrib. Mineral. Petrol.* **98**, 257-276.
- VRY, J.K., BROWN, P.E. & VALLEY, J.W. (1990): Cordierite volatile content and the role of CO₂ in high-grade metamorphism. *Am. Mineral.* **75**, 71-88.
- WICKHAM, S.M. (1987): The segregation and emplacement of granitic magmas. *J. Geol. Soc. London* **144**, 281-297.

Received August 18, 1993, revised manuscript accepted February 1, 1994.